Decoding auditory working memory content from intracranial high frequency activity in humans

Işıl Uluç * [1,2], Noam Peled [1,2], Angelique C. Paulk [3,4], Alan Bush [5,6], Valentina Gumenyuk [7], Parker Kotlarz [1], Kaisu Lankinen [1,2], Fahimeh Mamashli [1,2], Nao Matsuda [1], Mark R. Richardson [5,6], Steven M. Stufflebeam [1,2], Sydney S. Cash [3,4] & Jyrki Ahveninen [1,2]

[1] Athinoula A. Martinos Center for Biomedical Imaging, Department of Radiology, Massachusetts General Hospital, Charlestown, MA, USA

[2] Department of Radiology, Harvard Medical School, Boston, MA, USA

[3] Department of Neurology, Epilepsy Service, Massachusetts General Hospital, Boston, MA, USA

[4] Department of Neurology, Harvard Medical School, Boston, MA, USA

[5] Department of Neurosurgery, Massachusetts General Hospital, Boston, MA, USA

[6] Department of Neurosurgery, Harvard Medical School, Boston, MA, USA[7] University of Nebraska Medical Center, Omaha, NE, USA

Corresponding author *:
Işıl Uluç, Ph.D.
CNY 149, 13th St.
A.A. Martinos Center for Biomedical Imaging,
Department of Radiology,
Massachusetts General Hospital,
Charlestown, MA 02129
iuluc@mgh.harvard.edu
Tel: 617 726 6584, Fax: (617) 726-7422

Abstract

How the human brain maintains information in working memory (WM), a process critical for all our goal-directed function, has been debated for decades. Classic neurophysiological models, which argue that WM is maintained via persistent content-specific "delay activity," have been challenged by alternative ideas suggesting a combination of dynamic activity patterns and activity-silent mechanisms. Here, utilizing human intracranial stereo-EEG (sEEG) recordings and machine learning techniques, we tested understudied auditory WM in multiple cortical and subcortical brain areas. Neuronal activity was quantified as broadband high frequency activity (HFA, 70-190 Hz) which has been shown to be highly correlated with multiunit activity of neuron populations. Our multivariate pattern analysis (MVPA) results, validated via robust non-parametric permutation testing, show that information can be decoded from multiple brain regions, including prefrontal regions, superior temporal auditory cortices, and the hippocampus. However, the recording sites with high WM decoding accuracies were not accompanied by statistically significant increases in HFA power. In contrast, HFA power was reduced relative to the period preceding WM encoding in many frontal, superior temporal, and hippocampal sEEG recording sites. These results are in line with the hypothesis that WM maintenance can be supported by highly dynamic, "activity silent" processes rather than via persistent activity only.

Introduction

Working memory (WM), short term storage and manipulation of information, is crucial for goal-directed cognitive functions that enable us to maneuver the world. One of its behaviorally most relevant, and theoretically least understood, domains is auditory WM, a process essential for our ability to communicate, socialize, and operate with purpose in our dynamic everyday environments.

The neuronal mechanisms of WM have been a focus of intensive neuroscience research since the 1970's (Baddeley and Hitch, 1974; D'Esposito and Postle, 2015). Non-human primate (NHP) and non-invasive human imaging studies have given valuable insight into the brain networks underlying WM processing (Barak and Tsodyks, 2014; D'Esposito and Postle, 2015; Christophel et al., 2017; Constantinidis et al., 2018; Lundqvist et al., 2018). The emphasis of this research has been shifting from the "where" in the brain is WM maintained to the neurophysiological question "how" neurons carry information of WM content in the human brain (Barak and Tsodyks, 2014; D'Esposito and Postle, 2015; Stokes, 2015; Serences, 2016; Christophel et al., 2017; Miller et al., 2018).

The debate surrounding the nature of neuronal processes underlying WM maintenance started with the initial WM studies in NHP, showing that consistent firing in prefrontal cortex (PFC) accompanies WM retention, later on defined as delay activity (Fuster and Alexander, 1971; Rosenkilde et al., 1981). Neurophysiological studies suggested that such sustained delay activity patterns maintain information throughout the WM retention period (Goldman-Rakic, 1995; Romo et al., 1999; Constantinidis and Procyk, 2004; Vergara et al., 2016). The sustained firing was shown to be related to both excitatory and inhibitory dynamics of neurons (Barak and Tsodyks, 2014; Sreenivasan and D'Esposito, 2019). Subsequent human neuroimaging studies (Christophel et al., 2012; Christophel and Haynes, 2014; D'Esposito and Postle, 2015), however, showed that content-specific information could also be found in posterior brain areas where no sustained activity is present during WM maintenance. Evidence is also emerging that not only are posterior and sensory areas involved in WM maintenance but also the neuronal processes maintaining WM do not necessarily depend on persistently elevated neuronal firing. Some neurophysiological

studies in the auditory domain are consistent with this notion, suggesting that persistent delay-period spiking patterns, which were reported in certain early NHP and rodent studies (Gottlieb et al., 1989; Sakurai, 1990), do not necessarily carry information about the maintained content (Bigelow and Poremba, 2014; Ng et al., 2014; Scott et al., 2014).

The dichotomy between neurophysiological recordings in NHPs and human non-invasive studies has elicited different theories on the nature of the WM process, resulting in a reinterpretation of old findings regarding the persistent neuronal firing during the maintenance period. Several more recent neurophysiological studies support an interpretation that persistent firing during the WM delay period is a correlate of other brain functions including attention, decision-making, learning, or motor preparation (Lundqvist et al., 2018a; Sreenivasan and D'Esposito, 2019). At the same time, while the classic studies were based on trial-averaged signals, more recent studies using single-trial analysis approaches (Shafi et al., 2007; Lundqvist et al., 2016) suggest that WM is maintained via more dynamic process, involving sparse (rather than persistent) firing patterns and bursts of neuronal oscillations (Lundqvist et al., 2016; Kucewicz et al., 2017; Bastos et al., 2018; Lundqvist et al., 2018b). During the period between these bursts of activity, WM could be maintained in an “activity silent” state based on short-term synaptic plasticity (Mongillo et al., 2008; Stokes, 2015). However, these alternative theories have been criticized to be inconsistent with many neurophysiological findings regarding the neuronal underpinnings of WM (Constantinidis et al., 2018). For example, a limitation of the activity-silent models is that much of the experimental evidence (Wolff et al., 2015; Rose et al., 2016; Wolff et al., 2017b; Wolff et al., 2020; Mamashli et al., 2021) is coming mostly from non-invasive human studies (Constantinidis et al., 2018).

The insight about WM-related local neuronal circuits mostly come from NHP studies, primarily conducted in visual and tactile domains (Goldman-Rakic, 1995; Romo et al., 1999; Barak et al., 2010). Yet, the simple delayed-match-to-sample designs in highly trained laboratory animals are not optimal for differentiating between cognitive functions such as adaptive learning, long-term memory, and WM. This difficulty is, perhaps, most evident in the domain of auditory WM, as complex auditory-cognitive tasks are very difficult to learn for NHPs (Fritz et al., 2005; Scott et

al., 2012; Scott and Mishkin, 2016). In the auditory domain, this limitation leaves us mostly dependent on human neuroimaging studies (Lutzenberger et al., 2002; Kaiser et al., 2007; Kaiser, 2015; Kumar et al., 2016; Uluç et al., 2018; Ahveninen et al., 2023). One way to bridge the gap between NHP neurophysiological models and human neuroimaging studies is to use intracranial EEG recordings in human participants with epilepsy during their presurgical monitoring (Cash and Hochberg, 2015; Parvizi and Kastner, 2018).

Utilizing their high signal-to-noise ratio (SNR), human intracranial EEG studies provide direct access to neural correlates of WM compared to non-invasive neuroimaging or MEG/EEG recordings. For example, these studies have shown that the power of intracranial neuronal oscillations at the 30-60 Hz gamma band is modulated as a function of memory content during WM retention (Howard et al., 2003; Kaiser et al., 2008), whereas higher 65-120 Hz gamma was correlated with successful WM performance (Yamamoto et al., 2014). Most interestingly, intracranial recordings also provide access to > 70 Hz broadband high-frequency activity (HFA), which has been suggested to be a close correlate of local neuronal spiking (Ray et al., 2008; Leszczynski et al., 2020): Ray and colleagues (2008) showed a high temporal correlation between HFA and average firing rate in microelectrode recordings, suggesting that HFA is a correlate of multiunit activity (MUA) (although see also Leszczynski et al. 2020). Recent studies suggest that sustained patterns of HFA could play a role also in human WM processing, in line with the persistent firing model (Constantinidis et al., 2018). An open question, however, remains whether such WM-related HFA increases shown in humans reflect maintenance or executive processes aiding WM, such as attention.

Here, to examine neuronal mechanisms of WM in humans, we designed a retro-cue task to record neurophysiological signals from sEEG electrodes during auditory WM maintenance. Auditory tasks were utilized, not only because there are few neurophysiological studies relative to visual and tactile domains but also because auditory cortex is usually well sampled in sEEG implantations due to clinical considerations. In our task, we used auditory nonconceptual complex modulation patterns (ripple sounds) to ensure that the information maintained is nonverbal but has complex spectrotemporal features (for a more detailed explanation, see

Mamashli et al., 2021). We then decoded activity patterns from local field potential HFA patterns. To investigate the time course of the whole signal in more detail, we also decoded the information from intracranial event-related potentials (iERP) elicited during the maintenance period. Our results propose that WM content information is stored in HFA patterns from the bilateral superior temporal cortex (STC), hippocampus (HC), and inferior frontal gyrus (IFG). Based on these results, we suggest that HFA is a neural correlate of WM maintenance.

Methods

Participants

We collected stereo-EEG (sEEG) from thirteen participants (n=13, Female = 6, Male = 7; age=33.39±10.9 - ages are jittered for deidentification purposes) who were implanted mainly in frontal and temporal brain regions at Massachusetts General Hospital and Brigham and Women's Hospital. The participants had varying types of epilepsy with pharmaco-resistant complex partial seizures. Data of one participant was excluded due to insufficient number of trials. The data was collected while participants were undergoing invasive monitoring for epilepsy surgical evaluation. The electrode implantations were made exclusively based on clinical grounds as a part of diagnostic procedure. All participants provided written fully informed consent. Participants were informed that participation in the tests would not alter their clinical treatment and that they could withdraw at any time without jeopardizing their clinical care. The study design, protocol, and consent form were approved by the Mass General Brigham Institutional Review Board.

Stimuli and Procedure

Participants performed a retro-cue WM task with simultaneous recordings of behavior and sEEG from both cortical and subcortical brain structures. In our auditory WM experiment, we employed broadband sound patterns modulated across time (ripple velocity, ω cycles/s) and frequency (Ω cycles/octave) that are called ripple sounds as memory items. Ripple sounds were chosen as memoranda as they have speech-like patterns spectrotemporally (Shamma, 2001) but do not have conceptual properties (Fig. 1a). There were four 750-ms ripple sounds with different ripple velocities that were modified based on our previous studies (Mamashli et al., 2021; Ahveninen et al., 2023). To make the task feasible for our participants during their clinical stay, we determined the ripple velocities based on the largest just-noticeable-difference observed

among the participants in our previous study. The ripple velocities for the four item classes were 9.5, 18.2, 34.9, and 66.8 cycles/s. Two additional velocities were used for probes, including 5.0 and 128 cycles/s. Sound stimuli were delivered by loudspeakers (JBL Wireless Go 2, Harman I.I.Inc, USA or Cyber Acoustics Sound Bar USB Speaker, Cyber Acoustics inc., USA) externally connected to the task presentation computer.

The retro-cue WM paradigm, which is well established in the field (Christophel et al., 2012; Christophel and Haynes, 2014; Uluç et al., 2018; Ahveninen et al., 2023), aims to dissociate perception and attention from memory maintenance (Fig. 1b). It is essentially a modification of a delayed match to sample paradigm. In our WM task, we sequentially presented two 750-ms ripple sounds with a 250-ms interstimulus interval (ISI). The second ripple sound was followed by a retro-cue indicating the item to remember. The visual retro-cue consisted of a visual "memorize1" or "memorize2" cue- after another 250-ms ISI. After a 3-s maintenance period, in the middle of which an unrelated sound stimulus (50ms white noise)—i.e., an "impulse stimulus" (Wolff et al., 2017a) —was presented, a ripple sound probe was presented with a same/different response scheme. Participant gave a self-paced response by pressing A (same) and S (different) button presses on the keyboard, which were labeled respectively as "1" and "2", indicating if the test probe is the same as the memorized item or not. After each trial, a 1-s inter trial interval was registered (Fig. 1b).

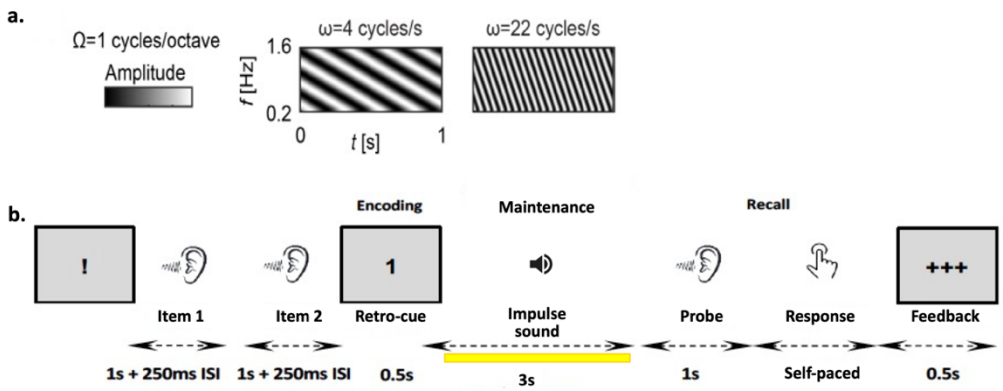

Figure 1. Diagram of the stimuli and paradigm. **(a)** Visualization of the spectrotemporal pattern of ripple sound stimuli. **(b)** Time course of the WM task. The presentation of ripple sounds is denoted by waves to the ears and the impulse sound iis denoted by an instrument. Participants were instructed to indicate if the probe matched the item indicated by the retro-cue via a button press in a self-paced manner and were provided with visual feedback.

Each run consisted of 24 trials, 12 of which were match and the remaining non-match. The non-match trials were divided into two parts with half the trials complete non-match trials where the probe was a different ripple sound from the two items that are presented at the beginning of the trial. The other half of the non-match trials designated the probe as the uncued item. The memory items were pseudo-randomly chosen from four different classes with different temporal frequencies. To eliminate categorical encoding, participants were naïve to the number of items to memorize. The task was planned to be 120 trials in total if completed with 5 runs. The number of trials completed changed across participants.

Data Acquisition

sEEG was recorded from a montage of 8-18 unilaterally or bilaterally implanted depth electrodes depending on the clinically indicated procedure per participant. Intracranial signals were recorded using a recording system with a sampling rate of 2000 Hz (Blackrock Microsystems, US) or with a sampling rate of 1024 Hz (Natus Quantum). At the time of acquisition, sEEG recordings were referenced to an EEG electrode that was placed on the head (either mastoid, cervical vertebrae 2, Cz or a sEEG contact that, based on imaging localization, was located in the skull and outside the brain).

Intracranial electrodes were localized by an established volumetric image co-registration procedure that is used for clinical application. First, the pre-operation T1-weighted MRI images were aligned to post-operation CT or MRI images that show electrode locations using Freesurfer scripts (http://surfer.mnr.mgh.harvard.edu). Electrode coordinates were manually determined from the post operation implant images. The electrodes were then mapped to standard cortical parcels/regions using the MMVT toolbox (Felsenstein et al., 2019; Soper et al., 2023).

The MMVT toolbox uses an automatic, probabilistic labeling algorithm that calculates the distances from and probability of each contact for each cortical and subcortical label using Electrodes Labeling Algorithm (ELA, https://github.com/pelednoam/ieil ; Peled et al., 2017). ELA identifies the nearest brain region label by creating an expanding cylinder around each electrode and calculating the probability of overlap of this cylinder with identified cortical and subcortical structure labels (Soper et al., 2023). We used the Lausanne500 parcellation atlas (Daducci et al., 2012) in addition to a subcortical mapping (Fischl et al., 2004; Desikan et al., 2006; Reuter et al., 2010; Reuter et al., 2012) for mapping the electrodes' locations. The electrodes that were within or less than 1.5 mm distance from cortical areas were taken as cortical electrodes. The electrodes within 2.5 mm distance from the centroid of the subcortical region were taken as subcortical electrodes. As our regions of interest, we chose Heschl's gyrus and superior temporal cortex (STC), the inferior frontal gyrus (IFG), and the hippocampus (HC), which have been previously related to WM maintenance (Leszczynski, 2011; Uluç et al., 2018; Mamashli et al., 2021). We also included the orbitofrontal gyrus (OFG) contacts because of its strong anatomical connection to

the monkey auditory cortex (Medalla and Barbas, 2014) and possible association with human auditory WM (Mamashli et al., 2021).

For the visualization of results in a common anatomical template, all contacts from all participants were resampled to Colin27-space using MMVT and ELA algorithm. Lausanne500 parcellation atlas and subcortical mapping was performed in the common space in the same manner as in native space.

Preprocessing

sEEG data was preprocessed with custom MATLAB scripts using the Fieldtrip toolbox (Oostenveld et al., 2011). The data was divided into single-trial epochs starting from 300 ms before to 3 s after the retro-cue onset. Bad channels as well as channels with excessive epileptiform activity and bad epochs were found and rejected based on visual evaluation. The data was detrended with a baseline window of -300 ms to 0 ms and filtered with a 300 Hz low pass and a 0.1 Hz high pass filter sequentially using *ft_preprocessing*. Notch filtering was used to remove 60 Hz line noise and its harmonics from the data. Blackrock datasets were downsampled to 1 kHz. Whole trial datasets were detrended and both European data format (EDF) and Blackrock format datasets were downsampled to 1 kHz. Data was then re-referenced to a common average of all remaining electrodes. After the spectral analysis, the outlier trials for each contact were calculated using MATLAB's built-in *isoutlier* function ('grubbs', threshold factor=1e-7) and contacts with more than 5 outlier trials were rejected from further analysis.

Main analyses

HFA Analysis

Epochs between -300 ms and 3 s with the onset at retro-cue were convolved with a dictionary of complex Morlet wavelets (each spanning seven cycles) at 2-Hz intervals between 70 Hz and 190

Hz for each contact for each trial. The frequency-specific sEEG power time series were then baseline corrected relative to the 300-ms pre-cue period and, finally, averaged across the frequency bins to yield the HFA time course for estimating content-specific patterns of brain activity during WM maintenance.

To examine the full trial HFA patterns, we calculated HFA time courses also across the entire 9-s trial period in the same fashion. The power was corrected to absolute baseline of 300 ms before the onset of the first sound item and averaged across frequency bins. HFA changes related to WM maintenance were estimated in each participant, contact, and time point using one-sample t-tests across individual trials. To ensure we do not miss any HFA increases that emerge during maintenance, the results are reported without conservative post hoc corrections. That is, the purpose was to avoid the Type II error that could be rejecting the persistent activity model due to using conservative thresholding. The results of these analyses were plotted as -log10(p) values, multiplied with the sign of the t in each time point and thresholded at $p<0.05$.

HFA Decoding Analysis

We employed a four-class classification with a support vector machine (SVM) classifier to decode the memorized items from sEEG HFA power during the WM maintenance. We utilized SVM implemented in libsvm (Chang and Lin, 2011) and provided in the COSMOMVPA package (Oosterhof et al., 2016) in MATLAB. SVM decoding accuracies were calculated based on median HFA power in sliding 500 ms windows (200 steps in the 3.3 s period, i.e., 16.5 ms steps) for each contact. To enhance the SNR, subaverages of four trials were calculated with each class using *cosmo_average_samples*. Fifty different random iterations were calculated of these subaveraged samples. Four-fold cross-validation was utilized for each iteration: the model was trained in 75% of the samples and tested in the remaining samples. *cosmo_nfold_partitioner* was used to ensure that the number of trials were balanced for each condition and the training and test data were separate. The decoding accuracies were averaged across the folds and iterations.

In the common space, a weighted decoding value is determined for each cortical label by the weighted average of participants with significant decoding accuracy for this cortical label. In the case where a participant had more than one contact with a significant decoding accuracy for this cortical label, we selected the contact with the highest decoding accuracy. We repeated this procedure for each time point in the maintenance period decoding analysis. For visual feasibility, 180 timepoint map figures were downsampled to 9 decoding accuracy maps throughout the maintenance period using sliding windows. The common space decoding accuracy maps were generated using MMVT.

Time-Domain intracranial event-related potentials (iERP) Decoding Analysis

As in HFA decoding, we employed a four-class SVM classification on the preprocessed signals from the sEEG electrodes. We calculated the SVM decoding accuracy using the temporal information within the 500-ms sliding time window at 20-ms steps. To enhance SNR, individual

trials were pooled to subaverages of 4 trials within each class using *cosmo_average_samples*. The same analysis was repeated across 50 random iterations of these subaveraged samples. Four-fold cross-validation was utilized for each iteration so that the model was trained in 75% of the samples and tested in the remaining 25% of the samples. The decoding accuracies were averaged across the folds and iterations.

Statistical Significance

Robust maximum-statistic permutation test strategy was utilized for dealing with multiple comparisons in the testing of decoding hypotheses. For both HFA and ERP decoding analyses, the statistical significance was calculated using a cluster-based maximum statistic permutation test with 500 permutations. The uncorrected cluster-forming threshold was determined non-parametrically: 99% of full distribution of decoding accuracies across all permutations in all contacts. We calculated the thresholds for each hemisphere separately because most participants were implanted unilaterally. Finally, the clusters of decoding accuracy over the threshold and a cluster-wise corrected p value were calculated for each electrode (containing 8-16 contacts).

Control Analyses

HFA Decoding Analysis on Uncued items

To control whether the SVM classification indicated memory information, we performed MVPA on HFA power for trials according to uncued items. The parameters for spectral analysis and SVM 4-class classification were the same as cued item analyses. The only difference was that the trials were defined according to the uncued item code.

Results

We studied human auditory WM using a ripple-sound retro-cue task in 12 participants under intracranial monitoring. Our multivariate pattern analyses suggested that maintained auditory WM content can be decoded from dynamic brain activation patterns, in the absence of persistently elevated activity relative to pre-trial baseline. WM content could be decoded from dynamic changes in broadband HFA, a putative correlate of concurrent firing activity, as well as from temporal patterns of intracranial event-related potentials (iERP).

Behavioral Performance

Participants (n=12) performed with 62.95±3.44 (mean±SEM) percent correct responses across all trials of a retro-cue paradigm. We performed an ANOVA with four levels to test if recall performance changes in relation to memorized ripple velocity. Our analysis showed no significant difference between the behavioral performance per memorized ripple velocity. Reaction time analysis could not be calculated due to the self-paced nature of the WM task.

iERP Analysis

The averaged voltages for the trial period showed responses to the sound stimuli, but no increase during maintenance period in the superior temporal contacts. In IFG contacts, the averages did not show any decrease or increase during WM stimuli presentations.

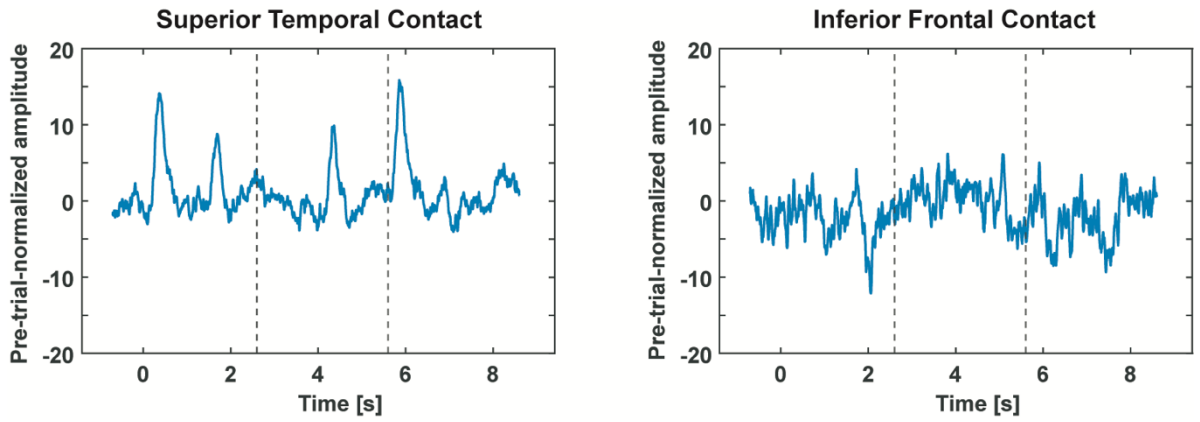

Figure 2. Examples of averaged iERP responses from two sEEG contacts from STC and IFG. The responses have been normalized based on the standard deviation of the pre-trial period. The WM maintenance period is between the vertical dashed lines.

Main Analyses

Figures 3-6 show the results of HFA analysis, four-class SVM classification of HFA and iERP in four brain areas that have previously been reported to maintain WM information in auditory (Uluç et al., 2018; Mamashli et al., 2021; Ahveninen et al., 2023) or other domains (Schmidt et al., 2015; Wu et al., 2018), including superior temporal cortex (STC; site of auditory cortex), the inferior frontal gyrus (IFG), and the hippocampus (HC). In addition, we also analyzed contacts within the orbitofrontal gyrus (OFG), given its strong domain-specific anatomical connectivity to the monkey auditory cortex (Medalla and Barbas, 2014) and possible association with human auditory WM (Mamashli et al., 2021).

Evidence for significant WM decoding results ($p<0.05$, maximum-statistic permutation test) using HFA data was found in all participants. SVM classification was applied to the medial power of HFA with a 500 ms sliding window from the 3.3-s maintenance period. In all analyses, the statistical

significance was calculated using a cluster-based maximum-statistic permutation test with 500 permutations.

Additionally, to investigate WM information embedded in the temporal fine structure of dynamic sEEG activity, we conducted a time-domain iERP classification analysis. In our four-class SVM classification, we used the temporal information of trial-specific iERP signals within sliding 500-ms across the WM maintenance period. In the iERP decoding analysis, as in the HFA decoding, we found WM information decodable from different cortical or subcortical contacts in all participants.

Complementary to decoding analyses, to examine maintenance related activation patterns, we analyzed the evolution of 70-190 Hz HFA, a putative correlate of local firing activity, in epochs encompassing the entire trial period. In this analysis, the signal power was compared to the period preceding the presentation (and encoding) of the first item. We especially wanted to explore if any continuous HFA would occur during periods where significant decoding could be shown.

The results are depicted below based on the pre-determined areas.

Auditory areas of Superior Temporal Cortex (STC)

Our STC analysis area includes contacts in Heschl's gyri (HG) and superior temporal gyri (STG): regions consisting primarily of primary/non-primary auditory cortices and auditory association areas. 10 out of the 12 participants had contacts in these areas. The significance for the decoding accuracies was calculated for each hemisphere separately because several of our participants had sEEG contacts implanted in only one hemisphere. Our HFA decoding sEEG contacts showed continuous clusters of significant decoding accuracy in 6 of these participants. In 4 of these participants, statistically significant above chance decoding accuracies spread throughout the whole maintenance period (Fig. 3d).

The temporal decoding analysis of the voltage responses showed significant decoding clusters in all 10 participants that had sEEG contacts in STC. Significant decoding results extended across the whole WM retention period in 6 of these 10 participants (Fig. 3e). Overall, significant decoding results were observed in a larger number of contacts in iERP than HFA decoding in STC. However, in HFA analysis, there was more evidence of significant decoding in a single contact across the entire maintenance period.

The significant decoding results were accompanied with no evidence of significant sustained elevation of HFA power in STC in contacts during maintenance period, even in uncorrected t-tests across trials. The only exception was the period following the “impulse sound” that is presented at 1.5 s into the maintenance period. In contrast to persistent increases, the HFA power was significantly decreased in most of the contacts (Fig. 3c).

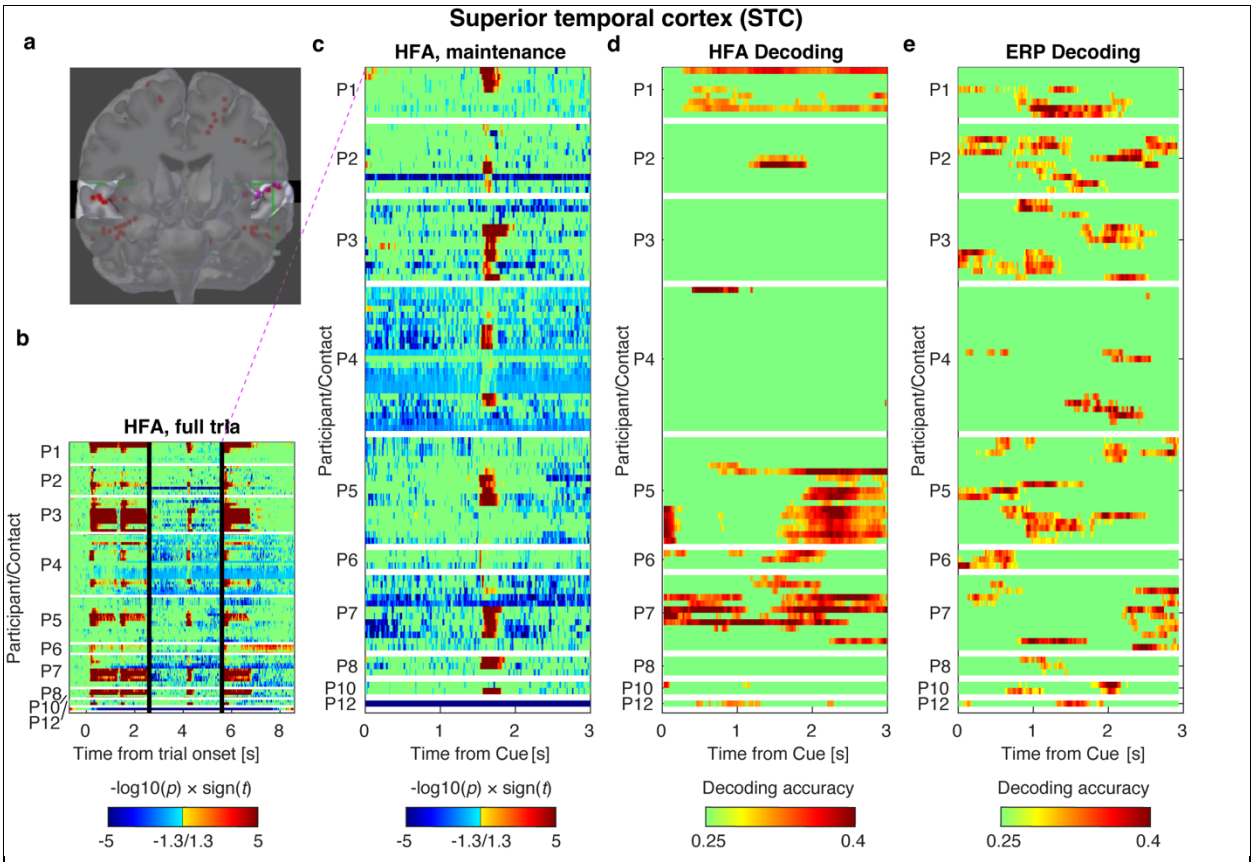

Figure 3 HFA time courses and WM decoding results in STC. **(a)** An example of contacts of electrodes that were implanted in STC. All results here are demonstrated for STC contacts within or less than 1.5 mm to the cortical label. **(b)** Whole trial HFA power time course. **(c)** Working memory period for HFA time courses. **(d)** HFA decoding analyses for STC contacts for all participants. **(e)** Time-domain decoding analysis from the iERP data. The decoding results have been thresholded based on a cluster-based maximum-statistic permutation test in each participant ($p<0.05$).

Inferior Frontal Gyrus (IFG)

All 12 participants had contacts in IFG. From these 12 participants, we found continuous clusters of significant decoding accuracies in 8 participants. However, for most of these contacts, the

significant clusters were either in the first half or the second half of the maintenance period only (Fig. 4d).

Significant iERP decoding results were, again, found in all 12 participants that had contacts in this area. In 5 of these participants, decoding results significantly above chance level extended across the entire 3-s maintenance period. In another 3 participants, significant results were very strongly present in either in the earlier or later part of the maintenance (Fig. 4e). Similar to the contact channels in AC, IFG channels in HFA had longer periods of continuous significant decoding accuracy.

Lateral PFC areas have historically been linked to WM maintenance via persistent firing activity (Funahashi et al., 1989; Constantinidis et al., 2018). We found evidence of sparse HFA increases in IFG. However, the general maintenance period of most of the contacts again was dominated by a reduction in power (Fig. 4c).

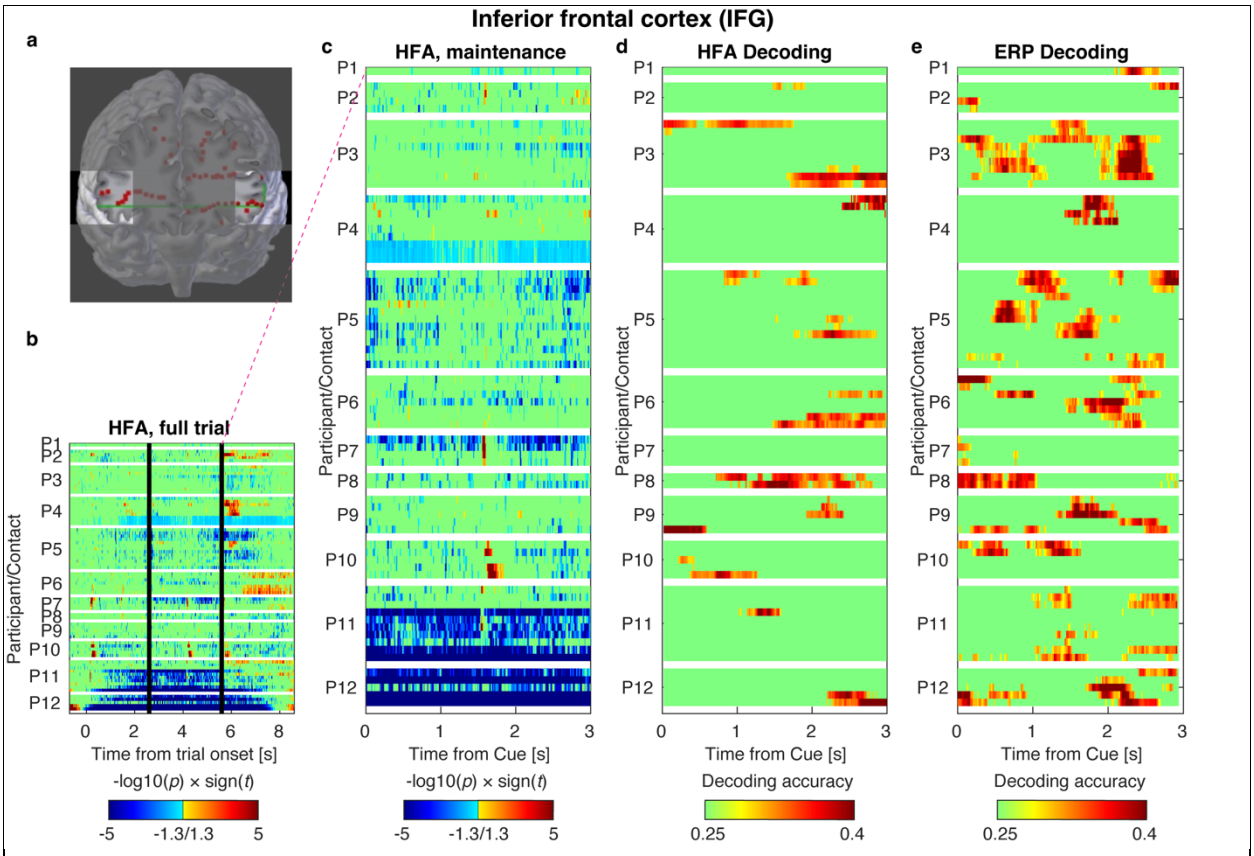

Figure 4. HFA time courses and WM decoding results in IFG. (**a)** An example of contacts in electrodes that were implanted in IFG. All results here are demonstrated for IFG contacts within or less than 1.5 mm to the cortical label. **(b)** Whole trial HFA power time course. **(c)** Working memory period for HFA time course. **(d)** HFA decoding analyses for IFG contacts for all participants. **(e)** Time-domain decoding analysis from the iERP data. The decoding results have been thresholded based on a maximum-statistic permutation test in each participant ($p<0.05$).

Orbitofrontal Gyrus (OFG)

Data from OFG contacts was available in 11 of our 12 participants. Although the number of recording contacts showing significant decoding accuracy within each participant was smaller for this region, 6 out of 11 participants had contacts that had continuous decoding clusters. Furthermore, 2 of those participants had decoding accuracies spread throughout the whole maintenance period in OFG contacts (Fig. 5d).

WM content could also be decoded from OFG in all 11 participants having contacts in this area. In 5 of these, significant decoding results emerged on and off throughout maintenance period (Fig. 5e). While the number of contacts showing significant results was larger than in iERP decoding, there was more evidence of significant results encompassing the entire maintenance period in one contact in HFA analysis in OFG.

OFG contacts also show HFA power elevation sparsely during maintenance, but we mostly observe reduction in HFA during WM maintenance across different contacts (Fig. 5c).

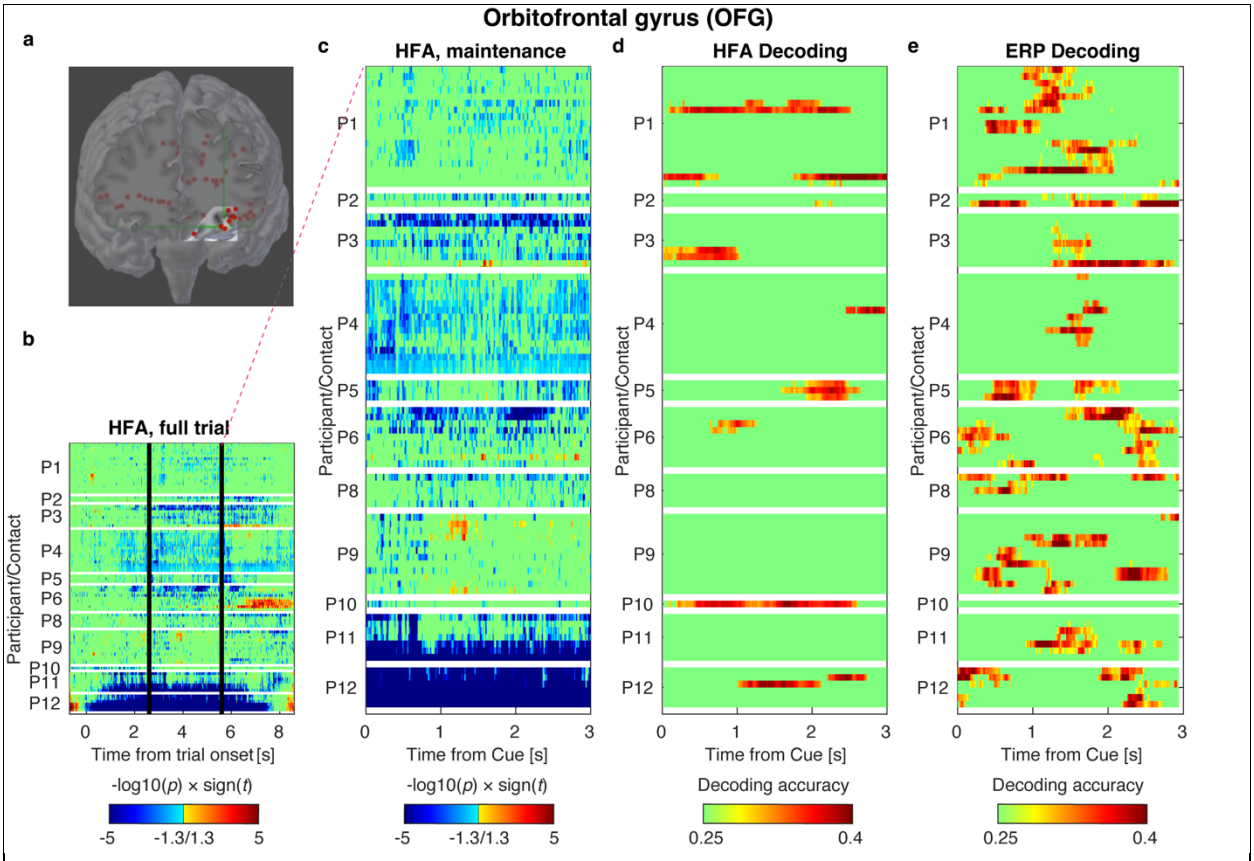

Figure 5. HFA time courses and WM decoding results in OFG. (**a)** example of electrodes that were implanted in OFG. All results here are demonstrated for IFG contacts within or less than 1.5 mm to the cortical label. **(b)** Whole trial HFA power time course. **(c)** Working memory period for HFA time course **(d)** HFA decoding analyses for OFG contacts for all participants **(e)** Time-domain decoding analysis from the iERP data. The decoding results have been thresholded based on a cluster-based maximum-statistic permutation test in each participant ($p<0.05$).

The Hippocampus (HC)

Data from contacts within HC was available from 11 out of the 12 participants. Out of these 10 participants, we observed significant decoding in 6 participants, with 4 of these participants showing significant decoding results during the entire maintenance period (Fig. 6d).

Finally, our SVM analysis on HC contacts revealed significant decoding in contacts in 8 out of 10 participants, 5 of which have contacts with over-chance decoding spread in the WM maintenance period (Fig. 6e). Comparison of these results to HFA decoding again presented contacts with longer significant accuracy periods in HFA classification.

HC contacts show a pattern consistent with other areas, exhibiting a decrease in power throughout the WM maintenance period (Fig. 6c).

For all the contacts that showed reduction in HFA power, none of them presented a similar pattern to the decoding accuracy patterns and were not always in channels with significant decoding accuracy.

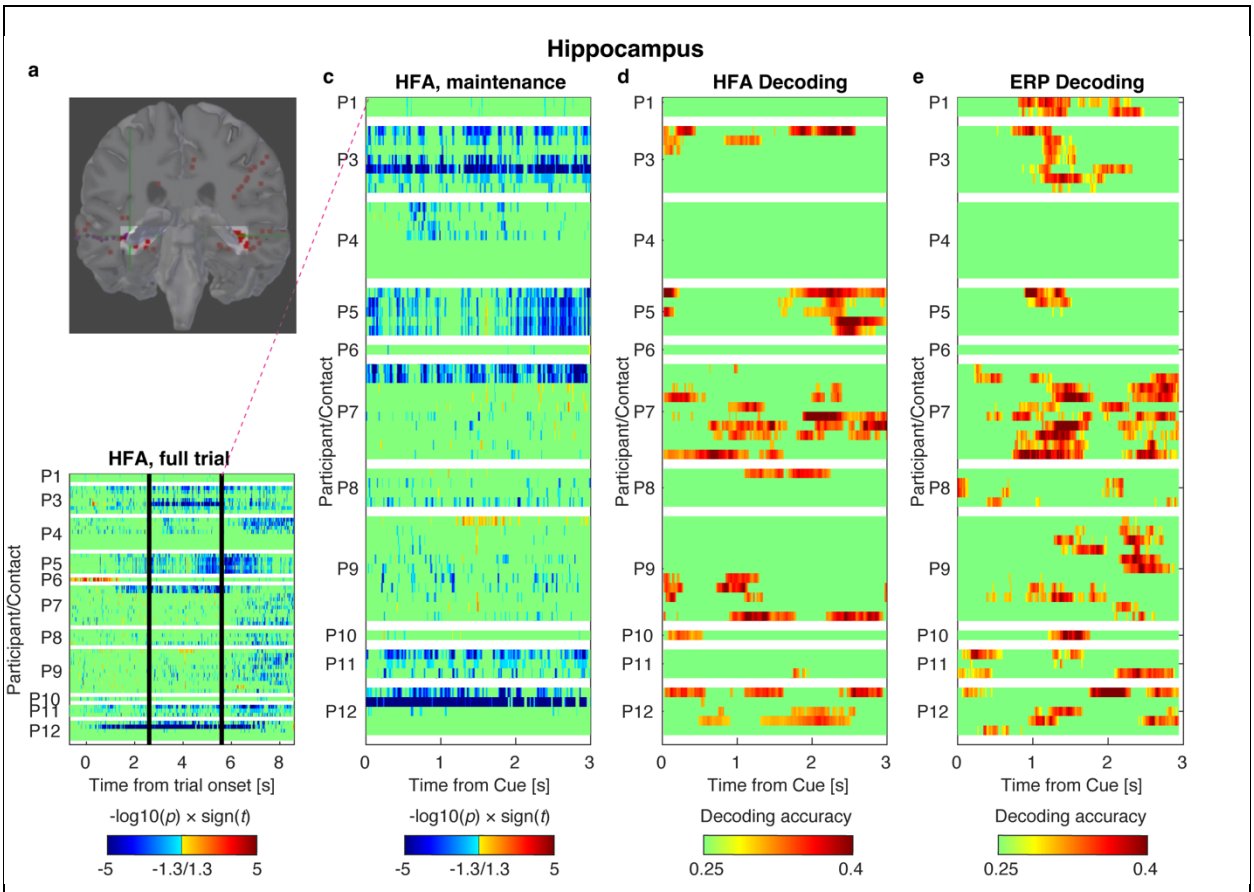

Figure 6. HFA time courses and WM decoding results in HC. (**a)** An example of contacts in electrodes that were implanted in HC. **(b)** Whole trial HFA power time course. **(c)** Working memory period for HFA time course. **(d)** HFA decoding analyses for IFG contacts for all participants **(e)** Time-domain decoding analysis from the iERP data. The decoding results have been thresholded based on a cluster-based maximum-statistic permutation test in each participant ($p<0.05$).

Decoding Results in Common Space

The HFA decoding results were plotted in a normalized Colin27-space as weighted averages of participant-contacts with significant decoding per label in a Laus500 parcellation atlas. Our widespread brain coverage (1180 cortical and subcortical contacts) findings demonstrated that

content-specific information is transient within the brain regions as well as spread across the cortical hierarchy (Fig. 7).

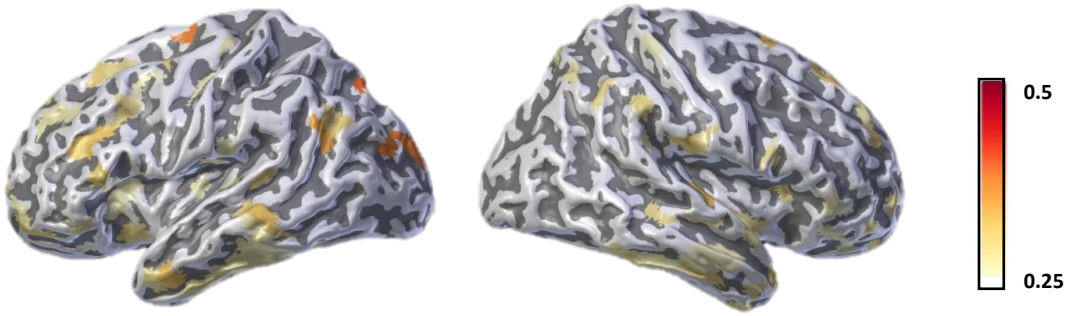

Figure 7. Whole brain weighted decoding averaged across whole WM period. The WM decoding accuracies were averaged across time and the weighted values were created as explained in *Methods subsection HFA Decoding Analysis.*

Control Analyses

HFA Decoding of Uncued memory items

As a control, we performed a four-class classification with an SVM classifier with the same parameters in the HFA decoding analysis on uncued stimuli. Our results showed no significant decoding in any of the relevant contacts.

Discussion

The focus of investigation in the mechanisms of WM has recently shifted from where the information is stored to what are the nature of processes that enable WM maintenance in humans (Lorenc and Sreenivasan, 2021). To this end, we employed intracranial sEEG depth electrode recordings to test whether the information is maintained by persistent activity or a more dynamic system of activities. We specifically examined whether WM representations are maintained via persistent elevation of neuronal activity or by a combination of more dynamic and activity-silent processes (Goldman-Rakic, 1995; Stokes, 2015) (for a discussion see, Lundqvist et al, 2018 and Constantinidis et al, 2018). In this context, we found evidence of content-specific WM representations carried by HFA, a putative correlate of multiunit firing activity, located in auditory, frontal areas, and hippocampal regions. Our temporal pattern decoding results, which examined WM content in 500-ms windows of unfiltered iERP voltage epochs, showed qualitatively similar decoding accuracy patterns from those areas. However, the HFA or temporal pattern decoding results, which were statistically significant according to our non-parametric permutation testing, were not accompanied with persistent increases of HFA power in comparison to the pre-trial baseline. Interestingly, in all areas of interest including higher order areas, in compliance with previous findings in the Romo laboratory (Barak and Tsodyks, 2014), HFA power significantly reduced in several contacts during WM maintenance, while the other contacts did not show any significant increase or decrease in HFA power. Most importantly, although some of the HFA power reduction could be denoted by the WM maintenance period, the spatiotemporal patterns of significant decoding and HFA power changes did not seem to overlap in any of our ROIs. These results are in line with an interpretation that WM maintenance is supported by a dynamic system which does not depend on persistent increases of neuronal activity in a specific brain region.

HFA has been proposed as a reliable indicator of population-level neuronal firing (i.e., MUA) in the immediate vicinity of intracranial depth electrode contacts (Ray et al., 2008; Ray and Maunsell, 2011; Leszczynski et al., 2020). Persistently elevated MUA patterns in PFC have, in turn, been proposed to be critical component for stable maintenance of WM maintenance (Fuster et

al., 2000; Mendoza-Halliday et al., 2014; Vergara et al., 2016; Constantinidis et al., 2018). Although the persistent firing model of WM does not assume stationary activity at the level of individual units, a proportion of neurons within the population that maintains WM should be active at least in a consistent pattern during the delay period (Constantinidis et al., 2018). In human sEEG, such population-level firing patterns should be visible as elevated patterns of HFA (Constantinidis et al., 2018). In contrast to this hypothesis, our results show little evidence of elevated HFA—stationary or non-stationary—in contacts showing evidence of content-specific HFA or iERP temporal patterns.

The present results are more closely consistent with a proposal that WM maintenance is a dynamic process, accompanied by a significant reduction in overall HFA during maintenance (Mongillo et al., 2008; Barak et al., 2010; Barak and Tsodyks, 2014; Lundqvist et al., 2018a). Our decoding results show that content-specific information can be decoded from multiple brain regions, some of which are frontal, auditory, and hippocampal regions. The information could be decoded in continuous chunks for a considerable part of the maintenance period. However, the WM decoding seems to fluctuate through time in these contacts. These stable but not uniform decoding accuracies suggest a more dynamic WM maintenance rather than processes consistently contained in localized neuronal populations (Stokes, 2015).

Robust decoding of WM content was found not only in frontal contacts but also in several of the STC contacts in or near auditory cortices. Consistent with the sensory recruitment model, we could decode content specific WM information from contacts both in earlier areas (HG, superior temporal plane) and in higher areas of lateral STG and STG/superior temporal sulcus (STS) boundary (Uluç et al., 2018; Mamashli et al., 2021; Ahveninen et al., 2023). The sensory recruitment model of WM has been countered with evidence that information-containing activation patterns sensory areas such as auditory cortex are not as resistant to intervening distractors than in higher areas (Xu, 2017). Indeed, in certain contacts of auditory cortex, we did observe that decoding drops to chance level during the strong feedforward activation pattern to the unrelated distractor (or “impulse” sound) (Fig 3c). However, in many of these contacts, the classifier performance rebounded after the strong feed-forward HFA to the impulse sound.

Impulse stimulus "perturbation" approaches have previously been utilized to address the challenge of evidencing activity silent dynamic states as neuronal underpinnings of WM maintenance (Wolff et al., 2015; Rose et al., 2016; Wolff et al., 2017b; Wolff et al., 2020; Mamashli et al., 2021). These "perturbation" studies have provided evidence that WM content maintained in an activity-silent state. That is, information could be decoded by examining content-specific changes to responses to these task-irrelevant impulse stimulus events. Compatible with these findings, in our study, some of auditory cortex contact channels showed significant decoding accuracy increase after impulse sound compatible with hidden state transitions that are coding WM information (Wolff et al., 2015; Rose et al., 2016; Wolff et al., 2017b; Wolff et al., 2020; Mamashli et al., 2021).

In addition to its well-documented role in episodic memory (Burgess et al., 2002; Moscovitch et al., 2016), a growing selection of studies provide evidence that HC could play a critical role in WM processing as well (Cabeza et al., 2002; Ezzyat and Olson, 2008; Axmacher et al., 2009; Leszczynski, 2011; Borders et al., 2022). Successful WM performance was shown to be correlated with increased gamma power in HC (Fell et al., 2001; Burgess and Ali, 2002). On the other hand, memory load in successfully remembered trials was correlated with a progressive HC suppression (Stretton et al., 2012). However, HC's role in WM processing has also been challenged by other earlier (Baddeley et al., 2011) and more recent (Slotnick, 2023) studies. Compatible with research showing HC to be an integral part of WM, our results also show involvement of hippocampus in WM maintenance (Fig. 6d). Our decoding analysis showed that WM information could be found in the HFA from contacts recording from HC. Borders and colleagues (2021) suggest that HC plays the precise role of supporting complex high-precision binding in WM. Our study design does not allow us to investigate the precision of auditory WM, but our analyses show that HC is involved in maintenance of complex sounds. In combination with the findings in other AC and frontal areas, our results point to a highly dynamic network distributed across several brain areas that is supported by activity silent processes as the neural correlate of WM maintenance.

Our results also suggest that some of the contacts from which we could decode WM content information show persistent suppression confined to the WM maintenance period. This is consistent with reports of several fMRI studies (Linke et al., 2011; Ahveninen et al., 2023; Deutsch et al., 2023) as well as with recent multi-site neurophysiological studies that reported suppressed firing in certain brain areas during maintenance (Dotson et al., 2018; Miller et al., 2018). Linke and colleagues have shown that instead of a robust content-specific activation, suppression in fMRI activity in sensory areas enable WM maintenance and dependent on the rehearsal strategy of the participant (Linke et al., 2011). They argue that the suppression might be a natural gatekeeping mechanism against distractors.

It should be noted that the sEEG method has limited coverage of the brain as the whole brain is not implanted with the sEEG electrodes. Hence, the activity of other regions contributing to WM maintenance cannot be ruled out. Furthermore, our HFA recordings reflect correlates but not direct measures of underlying neuronal activity (Leszczynski et al., 2020) and, as such, HFA does not allow us to rule out the role of more focal but persistent firing patterns in WM.

In conclusion, our study shows that neuronal processes underlying WM maintenance are highly dynamic processes that are spread across sensory and frontal areas as well as HC. These results are in line with the hypothesis that WM maintenance can be supported by highly dynamic activity silent processes rather than persistent activity.

References

Ahveninen J, Uluc I, Raij T, Nummenmaa A, Mamashli F (2023) Spectrotemporal content of human auditory working memory represented in functional connectivity patterns. Commun Biol 6:294.

Axmacher N, Elger CE, Fell J (2009) Working memory-related hippocampal deactivation interferes with long-term memory formation. J Neurosci 29:1052-1960.

Baddeley A, Jarrold C, Vargha-Khadem F (2011) Working memory and the hippocampus. J Cogn Neurosci 23:3855-3861.

Baddeley AD, Hitch G (1974) Working Memory. Psychology of Learning and Motivation 8:47-89.

Barak O, Tsodyks M (2014) Working models of working memory. Curr Opin Neurobiol 25:20-24.

Barak O, Tsodyks M, Romo R (2010) Neuronal population coding of parametric working memory. J Neurosci 30:9424-9430.

Bastos AM, Loonis R, Kornblith S, Lundqvist M, Miller EK (2018) Laminar recordings in frontal cortex suggest distinct layers for maintenance and control of working memory. Proc Natl Acad Sci U S A 115:1117-1122.

Bigelow J, Poremba A (2014) Achilles' ear? Inferior human short-term and recognition memory in the auditory modality. PLoS One 9:e89914.

Borders AA, Ranganath C, Yonelinas AP (2022) The hippocampus supports high-precision binding in visual working memory. Hippocampus 32:217-230.

Burgess N, Maguire EA, O'Keefe J (2002) The human hippocampus and spatial and episodic memory. Neuron 35:625-641.

Cabeza R, Dolcos F, Graham R, Nyberg L (2002) Similarities and differences in the neural correlates of episodic memory retrieval and working memory. Neuroimage 16:317-330.

Chang C-C, Lin C-J (2011) LIBSVM: A library for support vector machines. ACM Trans Intell Syst Technol 2:1-27.

Christophel TB, Haynes JD (2014) Decoding complex flow-field patterns in visual working memory. NeuroImage 91:43-51.

Christophel TB, Hebart MN, Haynes J-D (2012) Decoding the contents of visual short-term memory from human visual and parietal cortex. The Journal of neuroscience : the official journal of the Society for Neuroscience 32:12983-12989.

Christophel TB et al. (2017) The Distributed Nature of Working Memory. Trends in Cognitive Sciences 0:115-142.

Constantinidis C, Procyk E (2004) The primate working memory networks. Cogn Affect Behav Neurosci 4:444-465.

Constantinidis C, Funahashi S, Lee D, Murray JD, Qi XL, Wang M, Arnsten AFT (2018) Persistent Spiking Activity Underlies Working Memory. J Neurosci 38:7020-7028.

D'Esposito M, Postle BR (2015) The Cognitive Neuroscience of Working Memory. Annual Review of Psychology 66:115-142.

Daducci A, Gerhard S, Griffa A, Lemkaddem A, Cammoun L, Gigandet X, Meuli R, Hagmann P, Thiran JP (2012) The connectome mapper: an open-source processing pipeline to map connectomes with MRI. PLoS One 7:e48121.

Desikan RS, Segonne F, Fischl B, Quinn BT, Dickerson BC, Blacker D, Buckner RL, Dale AM, Maguire RP, Hyman BT, Albert MS, Killiany RJ (2006) An automated labeling system for subdividing the human cerebral cortex on MRI scans into gyral based regions of interest. Neuroimage 31:968-980.

Deutsch P, Czoschke S, Fischer C, Kaiser J, Bledowski C (2023) Decoding of Working Memory Contents in Auditory Cortex Is Not Distractor-Resistant. J Neurosci 43:3284-3293.

Dotson NM, Hoffman SJ, Goodell B, Gray CM (2018) Feature-Based Visual Short-Term Memory Is Widely Distributed and Hierarchically Organized. Neuron 99:215-226 e214.

Ezzyat Y, Olson IR (2008) The medial temporal lobe and visual working memory: comparisons across tasks, delays, and visual similarity. Cogn Affect Behav Neurosci 8:32-40.

Fischl B, van der Kouwe A, Destrieux C, Halgren E, Segonne F, Salat DH, Busa E, Seidman LJ, Goldstein J, Kennedy D, Caviness V, Makris N, Rosen B, Dale AM (2004) Automatically parcellating the human cerebral cortex. Cereb Cortex 14:11-22.

Fritz J, Mishkin M, Saunders RC (2005) In search of an auditory engram. Proc Natl Acad Sci U S A 102:9359-9364.

Funahashi S, Bruce CJ, Goldman-Rakic PS (1989) Mnemonic coding of visual space in the monkey's dorsolateral prefrontal cortex. Journal of Neurophysiology 61:331-349.

Fuster JM, Alexander GE (1971) Excitation and Inhibition of Neuronal Firing in Visual Cortex by Reticular Stimulation. Science 133:2011-2012.

Fuster JM, Bodner M, Kroger JK (2000) Cross-modal and cross-temporal association in neurons of frontal cortex. Nature 405:347-351.

Goldman-Rakic PS (1995) Cellular basis of working memory. Neuron 14:477-485.

Gottlieb Y, Vaadia E, Abeles M (1989) Single unit activity in the auditory cortex of a monkey performing a short term memory task. Exp Brain Res 74:139-148.

Howard MW, Rizzuto DS, Caplan JB, Madsen JR, Lisman J, Aschenbrenner-Scheibe R, Schulze-Bonhage A, Kahana MJ (2003) Gamma oscillations correlate with working memory load in humans. Cereb Cortex 13:1369-1374.

Kaiser J (2015) Dynamics of auditory working memory. Front Psychol 6:613.

Kaiser J, Heidegger T, Wibral M, Altmann CF, Lutzenberger W (2007) Alpha synchronization during auditory spatial short-term memory. Neuroreport 18:1129-1132.

Kaiser J, Heidegger T, Wibral M, Altmann CF, Lutzenberger W (2008) Distinct gamma-band components reflect the short-term memory maintenance of different sound lateralization angles. Cereb Cortex 18:2286-2295.

Kucewicz MT, Berry BM, Kremen V, Brinkmann BH, Sperling MR, Jobst BC, Gross RE, Lega B, Sheth SA, Stein JM, Das SR, Gorniak R, Stead SM, Rizzuto DS, Kahana MJ, Worrell GA (2017) Dissecting gamma frequency activity during human memory processing. Brain 140:1337-1350.

Kumar S, Joseph S, Gander PE, Barascud N, Halpern AR, Griffiths TD (2016) A Brain System for Auditory Working Memory. The Journal of neuroscience : the official journal of the Society for Neuroscience 36:4492-4505.

Leszczynski M (2011) How does hippocampus contribute to working memory processing? Front Hum Neurosci 5:168.

Leszczynski M, Barczak A, Kajikawa Y, Ulbert I, Falchier AY, Tal I, Haegens S, Melloni L, Knight RT, Schroeder CE (2020) Dissociation of broadband high-frequency activity and neuronal firing in the neocortex. Sci Adv 6:eabb0977.

Linke AC, Vicente-Grabovetsky A, Cusack R (2011) Stimulus-specific suppression preserves information in auditory short-term memory. Proceedings of the National Academy of Sciences of the United States of America 108:12961-12966.

Lundqvist M, Herman P, Miller EK (2018a) Working Memory: Delay Activity, Yes! Persistent Activity? Maybe Not. J Neurosci 38:7013-7019.

Lundqvist M, Herman P, Warden MR, Brincat SL, Miller EK (2018b) Gamma and beta bursts during working memory readout suggest roles in its volitional control. Nat Commun 9:394.

Lundqvist M, Rose J, Herman P, Brincat SL, Buschman TJ, Miller EK (2016) Gamma and Beta Bursts Underlie Working Memory. Neuron 90:152-164.

Lutzenberger W, Ripper B, Busse L, Birbaumer N, Kaiser J (2002) Dynamics of gamma-band activity during an audiospatial working memory task in humans. J Neurosci 22:5630-5638.

Mamashli F, Khan S, Hamalainen M, Jas M, Raij T, Stufflebeam SM, Nummenmaa A, Ahveninen J (2021) Synchronization patterns reveal neuronal coding of working memory content. Cell Rep 36:109566.

Medalla M, Barbas H (2014) Specialized prefrontal "auditory fields": organization of primate prefrontal-temporal pathways. Front Neurosci 8:77.

Mendoza-Halliday D, Torres S, Martinez-Trujillo JC (2014) Sharp emergence of feature-selective sustained activity along the dorsal visual pathway. Nature Neuroscience 17:1255-1262.

Miller EK, Lundqvist M, Bastos AM (2018) Working Memory 2.0. Neuron 100:463-475.

Mongillo G, Barak O, Tsodyks M (2008) Synaptic theory of working memory. Science 319:1543-1546.

Moscovitch M, Cabeza R, Winocur G, Nadel L (2016) Episodic Memory and Beyond: The Hippocampus and Neocortex in Transformation. Annu Rev Psychol 67:105-134.

Ng CW, Plakke B, Poremba A (2014) Neural correlates of auditory recognition memory in the primate dorsal temporal pole. J Neurophysiol 111:455-469.

Oostenveld R, Fries P, Maris E, Schoffelen JM (2011) FieldTrip: Open source software for advanced analysis of MEG, EEG, and invasive electrophysiological data. Comput Intell Neurosci 2011:156869.

Oosterhof NN, Connolly AC, Haxby JV (2016) CoSMoMVPA: Multi-Modal Multivariate Pattern Analysis of Neuroimaging Data in Matlab/GNU Octave. Front Neuroinform 10:27.

Parvizi J, Kastner S (2018) Promises and limitations of human intracranial electroencephalography. Nat Neurosci 21:474-483.

Ray S, Maunsell JH (2011) Different origins of gamma rhythm and high-gamma activity in macaque visual cortex. PLoS Biol 9:e1000610.

Ray S, Crone NE, Niebur E, Franaszczuk PJ, Hsiao SS (2008) Neural correlates of high-gamma oscillations (60-200 Hz) in macaque local field potentials and their potential implications in electrocorticography. J Neurosci 28:11526-11536.

Reuter M, Rosas HD, Fischl B (2010) Highly accurate inverse consistent registration: a robust approach. Neuroimage 53:1181-1196.

Reuter M, Schmansky NJ, Rosas HD, Fischl B (2012) Within-subject template estimation for unbiased longitudinal image analysis. Neuroimage 61:1402-1418.

Romo R, Brody CD, Hernández A, Lemus L (1999) Neuronal correlates of parametric working memory in the prefrontal cortex. Nature 399:470-473.

Rose NS, LaRocque JJ, Riggall AC, Gosseries O, Starrett MJ, Meyering EE, Postle BR (2016) Reactivation of latent working memories with transcranial magnetic stimulation. Science 354:1136-1139.

Rosenkilde CE, Bauer RH, Fuster JM (1981) Single cell activity in ventral prefrontal cortex of behaving monkeys. Brain Res 209:375-394.

Sakurai Y (1990) Hippocampal cells have behavioral correlates during the performance of an auditory working memory task in the rat. Behav Neurosci 104:253-263.

Schmidt TT, Wu Y-h, Blankenburg F (2015) Print |Close PFC maintains abstract quantitative but not spatial tactile stimulus features during working memory. In: OHBM 2015.

Scott BH, Mishkin M (2016) Auditory short-term memory in the primate auditory cortex. Brain Res 1640:264-277.

Scott BH, Mishkin M, Yin P (2012) Monkeys have a limited form of short-term memory in audition. Proc Natl Acad Sci U S A 109:12237-12241.

Scott BH, Mishkin M, Yin P (2014) Neural correlates of auditory short-term memory in rostral superior temporal cortex. Curr Biol 24:2767-2775.

Shafi M, Zhou Y, Quintana J, Chow C, Fuster J, Bodner M (2007) Variability in neuronal activity in primate cortex during working memory tasks. Neuroscience 146:1082-1108.

Serences JT (2016) Neural mechanisms of information storage in visual short-term memory. Vision Research 128:53-67.

Shamma S (2001) On the role of space and time in auditory processing. Trends Cogn Sci 5:340-348.

Soper DJ, Reich D, Ross A, Salami P, Cash SS, Basu I, Peled N, Paulk AC (2023) Modular pipeline for reconstruction and localization of implanted intracranial ECoG and sEEG electrodes. PLoS One 18:e0287921.

Sreenivasan KK, D'Esposito M (2019) The what, where and how of delay activity. Nat Rev Neurosci 20:466-481.

Slotnick SD (2023) No convincing evidence the hippocampus is associated with working memory. Cogn Neurosci 14:96-106.

Stokes MG (2015) 'Activity-silent' working memory in prefrontal cortex: a dynamic coding framework. Trends Cogn Sci 19:394-405.

Uluç I, Schmidt TT, Wu YH, Blankenburg F (2018) Content-specific codes of parametric auditory working memory in humans. NeuroImage 183.

Vergara J, Rivera N, Rossi-Pool R, Romo R (2016) A Neural Parametric Code for Storing Information of More than One Sensory Modality in Working Memory. Neuron 89:54-62.

Wolff MJ, Ding J, Myers NE, Stokes MG (2015) Revealing hidden states in visual working memory using electroencephalography. Front Syst Neurosci 9:123.

Wolff MJ, Jochim J, Akyurek EG, Stokes MG (2017) Dynamic hidden states underlying working-memory-guided behavior. Nat Neurosci 20:864-871.

Wolff MJ, Kandemir G, Stokes MG, Akyurek EG (2020) Unimodal and Bimodal Access to Sensory Working Memories by Auditory and Visual Impulses. J Neurosci 40:671-681.

Wu Y-h, Uluç I, Schmidt TT, Tertel K, Kirilina E, Blankenburg F (2018) Overlapping frontoparietal networks for tactile and visual parametric working memory representations. NeuroImage 166:325-334.

Xu Y (2017) Reevaluating the Sensory Account of Visual Working Memory Storage. Trends Cogn Sci 21:794-815.

Yamamoto J, Suh J, Takeuchi D, Tonegawa S (2014) Successful execution of working memory linked to synchronized high-frequency gamma oscillations. Cell 157:845-857.

Barak O, Tsodyks M (2014) Working models of working memory. Curr Opin Neurobiol 25:20-24.

Burgess AP, Ali L (2002) Functional connectivity of gamma EEG activity is modulated at low frequency during conscious recollection. Int J Psychophysiol 46:91-100.

Cash SS, Hochberg LR (2015) The emergence of single neurons in clinical neurology. Neuron 86:79-91.

Christophel TB et al. (2017) The Distributed Nature of Working Memory. Trends in Cognitive Sciences 0:115-142.

Constantinidis C, Funahashi S, Lee D, Murray JD, Qi XL, Wang M, Arnsten AFT (2018) Persistent Spiking Activity Underlies Working Memory. J Neurosci 38:7020-7028.

D'Esposito M, Postle BR (2015) The Cognitive Neuroscience of Working Memory. Annual Review of Psychology 66:115-142.

Fell J, Klaver P, Lehnertz K, Grunwald T, Schaller C, Elger CE, Fernandez G (2001) Human memory formation is accompanied by rhinal-hippocampal coupling and decoupling. Nat Neurosci 4:1259-1264.

Funahashi S, Bruce CJ, Goldman-Rakic PS (1989) Mnemonic coding of visual space in the monkey's dorsolateral prefrontal cortex. Journal of Neurophysiology 61:331-349.

Leszczynski M (2011) How does hippocampus contribute to working memory processing? Front Hum Neurosci 5:168.

Leszczynski M, Barczak A, Kajikawa Y, Ulbert I, Falchier AY, Tal I, Haegens S, Melloni L, Knight RT, Schroeder CE (2020) Dissociation of broadband high-frequency activity and neuronal firing in the neocortex. Sci Adv 6:eabb0977.

Lundqvist M, Herman P, Miller EK (2018) Working Memory: Delay Activity, Yes! Persistent Activity? Maybe Not. J Neurosci 38:7013-7019.

Mamashli F, Khan S, Hamalainen M, Jas M, Raij T, Stufflebeam SM, Nummenmaa A, Ahveninen J (2021) Synchronization patterns reveal neuronal coding of working memory content. Cell Rep 36:109566.

Miller EK, Lundqvist M, Bastos AM (2018) Working Memory 2.0. Neuron 100:463-475.

Mongillo G, Barak O, Tsodyks M (2008) Synaptic theory of working memory. Science 319:1543-1546.

Parvizi J, Kastner S (2018) Promises and limitations of human intracranial electroencephalography. Nat Neurosci 21:474-483.

Rose NS, LaRocque JJ, Riggall AC, Gosseries O, Starrett MJ, Meyering EE, Postle BR (2016) Reactivation of latent working memories with transcranial magnetic stimulation. Science 354:1136-1139.

Serences JT (2016) Neural mechanisms of information storage in visual short-term memory. Vision Research 128:53-67.

Slotnick SD (2023) No convincing evidence the hippocampus is associated with working memory. Cogn Neurosci 14:96-106.

Sreenivasan KK, D'Esposito M (2019) The what, where and how of delay activity. Nat Rev Neurosci 20:466-481.

Stokes MG (2015) 'Activity-silent' working memory in prefrontal cortex: a dynamic coding framework. Trends Cogn Sci 19:394-405.

Stretton J, Winston G, Sidhu M, Centeno M, Vollmar C, Bonelli S, Symms M, Koepp M, Duncan JS, Thompson PJ (2012) Neural correlates of working memory in Temporal Lobe Epilepsy--an fMRI study. Neuroimage 60:1696-1703.

Uluç I, Schmidt TT, Wu YH, Blankenburg F (2018) Content-specific codes of parametric auditory working memory in humans. NeuroImage 183.

Wolff MJ, Ding J, Myers NE, Stokes MG (2015) Revealing hidden states in visual working memory using electroencephalography. Front Syst Neurosci 9:123.

Wolff MJ, Jochim J, Akyurek EG, Stokes MG (2017a) Dynamic hidden states underlying working-memory-guided behavior. Nat Neurosci 20:864-871.

Wolff MJ, Jochim J, Akyurek EG, Stokes MG (2017b) Dynamic hidden states underlying working-memory-guided behavior. Nat Neurosci.

Wolff MJ, Kandemir G, Stokes MG, Akyurek EG (2020) Unimodal and Bimodal Access to Sensory Working Memories by Auditory and Visual Impulses. J Neurosci 40:671-681.